

indirectly on the resistivity, which is a parameter of the permeability ($\hat{\mu}_{sk}$). Furthermore, by reducing the thickness of the sample, it is possible to reduce the degree of variation in the induced voltage values due to the resistivity. Therefore, it is possible to monitor the development of the nitride layer by using magnetic sensors by monitoring the change in voltage generated in the coil [16]. In the early stages of nitrided layer formation, nitrogen diffusion induces the expansion of the surface layer of the material. This expansion is being resisted by the rest of the material with smaller concentrations of nitrogen. The macro stress characteristic developed as a result of the process for those specimens, from the diffusion point, to the finite thickness, these stresses can be described by following equation [4]:

$$\sigma_{(x,t)} = \frac{\beta \cdot E}{1 - \nu} \left\{ \overline{[N(t)]} - [N(x,t)] \right\} \quad (9)$$

where: $\sigma_{(x,t)}$ – macrostresses which are parallel to the surface, in x distance from the surface, β - Vegard constant, E - Young's modulus, ν - Poisson constant, $[N(t)]$ - average nitrogen concentration in sample in t time of process, $[N(x,t)]$ - surface nitrogen concentration in x distance from surface in t time of process. Due to the fact that the expansion of the lattice caused by the diffusion of nitrogen is positive ($\beta > 0$), it follows the equation near the surface, with the compression stress $\{[N(t)] < [N(x,t)]\}$, while tensile stress exists in areas farther from the surface where $\{[N(t)] > [N(x,t)]\}$. The above formulas show that when there is a change in the structure and concentration of nitrogen atoms over time, the formation of the macro stress can be simulated and calculated. Thus, the value of the voltage change in the sensor can be compared to the change in the magnetic stress by a function over time. At the same time, it is possible to determine the nitrogen concentration by solving the diffusion problems under Fick's law and form permeable layers. This means that the atomic nitrogen concentration on the surface reaches the equilibrium value with the nitrogen concentration inside the permeation medium.

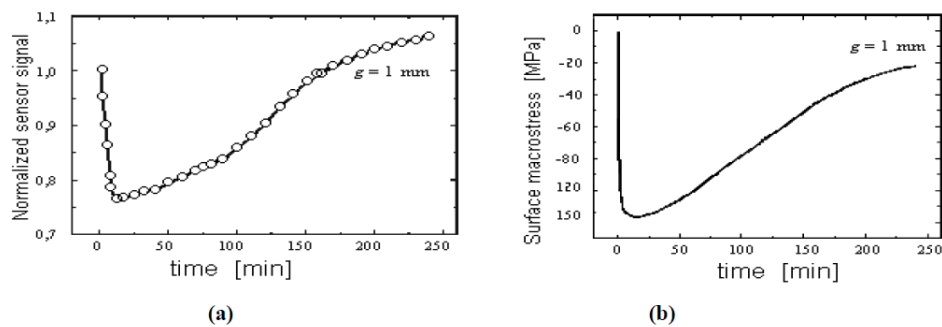


Figure 11: (a) Variation in sensor signal (magnetising current frequency $f = 150$ kHz) as a function of nitriding time for an iron specimen of thickness $g = 1$ mm. (b) Calculated changes of surface compressive macrostress in an iron specimen of thickness $g = 1$ mm; process parameters: $T = 560^\circ\text{C}$ (833 K), $KN = 0.08$ [37].

Figure 11a shows an example of changes in the voltage induced in a magnetic sensor during nitrogen adsorption to a 1 mm thick steel sample. Samples were placed in infiltration medium with $KN = 0.08$ permeability at 560°C . The registered properties $U = f(t)$ correspond to the qualitative significance for the change of surface macro stresses (Figure 11b) as calculated for the above parameters of the process. These macro stresses represent the two characteristic phases of diffusion. Previously connected with an increase in surface nitrogen concentration accompanied by an increase in compression pressure and a decrease in the voltage signal, in

the case of the later stage there is relaxation of the stress, increasing the voltage [43,44].

6. DESIGN AND CONSTRUCTION OF MAGNETIC SENSOR

The basic part of the measuring system, *i.e.*, the magnetic sensor, is placed in a furnace retort, cf. Figure 12. This is a run-through sensor: the gas nitriding atmosphere flows through it and causes the formation of a nitride layer on the specimen placed inside the sensor.

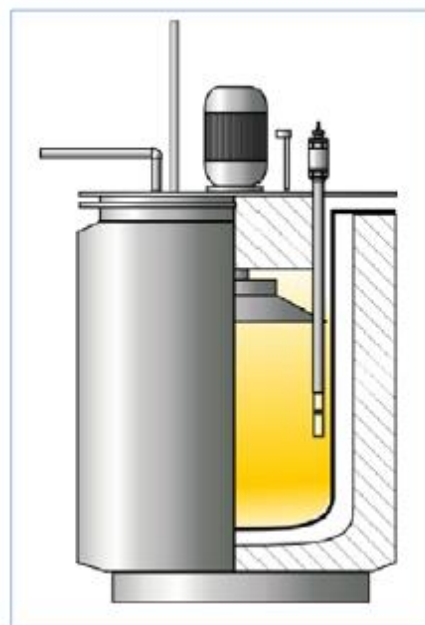


Figure 12: Magnetic sensor placed in furnace retort

Structure and principle of operation of the hydrogen sensor is shown in Figure 13 and Figure 14.



Figure 13: Hydrogen sensor

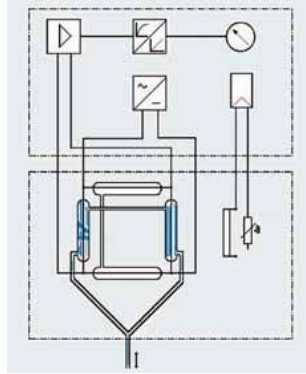


Figure 14: Diagram of hydrogen sensor

The hydrogen sensor consists of a Wheatstone bridge of four temperature dependent resistors. Two parallel resistors placed in the gas need to be analyzed, the other two resistors in a stable gas environment that know exactly the thermal conductivity. During the measurement, all four resistors were heated to above 500°C. The thermal conductivity of gases in the environment depends primarily on the hydrogen content. Therefore, the resistance in the test chamber will change linearly with temperature. The more hydrogen-rich the environment, the smaller the metal resistance, so the more electrical current it needs to get to zero. This current is proportional to the measured hydrogen concentration. The device measures from 0% H₂ with 4mA to 75% H₂ with 20mA. Based on the change of the current signal, the H₂ concentration of the medium is determined. The hydrogen sensor is used to measure the gas outside the furnace with the following specifications:

- + H₂ concentration measurement: 0 - 75%.
- + Supply voltage: 24 V, using DC source.
- + Output current: 4- 20 mA.
- + Retention time: Output delay 6 ... 20s

This sensor operates in all temperature ranges with high reliability. The electronic evaluation and current system integrated in the sensor. Bring a compact design and simple connectivity. The interference effects of other gases such as O₂, N₂, CO, H₂O and CO₂ are automatically compensated. Thus, only one type of sensor for all gas mixtures may be required. The hydrogen sensor can be measured in nitrogen.

7. CONCLUSION

This paper introduces the nitriding technology as well as some knowledge of sensor permeability, particularly the hydrogen sensor. The authors studied about nitriding technology and methods for controlling the permeability process as well as the use of hydrogen sensors in controlling the nitriding process.

REFERENCES

- [1] ASM Handbook Vo 1 published 2005. Properties Selection of Iron and Steels.
- [2] ASM Handbook Vo 9 published 2004. Metallography and Microstructure.
- [3] ASM Handbook Vo 4 published 2002. Failure Analysis and Prevention.
- [4] ASM, Heat treating, Vol 4, 2011.
- [5] Le, T.N., Pham, M.K., Hoang, A.T., Bui, T.N.M., Nguyen, D.N. 2018. Microstructure change for multi-pass welding between austenitic stainless steel and carbon steel. *Journal of Mechanical Engineering Research & Developments*, 41(2), 97-102.
- [6] Le, T.N., Pham, M.K., Hoang, A.T., Nguyen, D.N. 2018. Microstructure and elements distribution in the transition zone of carbon steel and stainless-steel welds. *Journal of Mechanical Engineering Research and Developments*, 41 (3), 27-31.
- [7] Pham, M.K., Nguyen, D.N., Hoang, A.T. 2018. Influence of Vanadium on the Microstructure and Mechanical Properties of High-Manganese steel. *International Journal of Mechanical and Mechatronics Engineering*, 18 (2), 141-147.
- [8] Lakhtin, Y.M. 1977. (Translated from Russian by Nicholá Weinstein) *Engineering physical metallurgy and heat-treatment*; Mir publishers. Moscow.
- [9] Polat, S., Atapek, H., Gumus, P. 2012. *International Iron and Steel Symposium 02-04 April Tarabuk Turkey: Gas nitriding hot work Tool Steel and its characterization*.
- [10] Ben, S. 2012. Sliama Reseach Unit Material Engineering National Engineering School of Tunis Tunisia 10th: Iron and Gas Nitriding Applied to Steel Tool Hot Work X38CrMoV5 Nitriding Impact on the Wear August.
- [11] Farkas, D., Ohla, K. 1933. *Modeling of Diffusion Processes During Carburization of Alloys, Oxidation of Metals*, 19.
- [12] Jimenez, H., Staia, M.H., Puchi, E.S. 1999. Mathematical modeling of a carburizing process of a SAE 3630H steel. *Surface and Coatings Technology*, 130-131, 353-365.
- [13] Hoang, A.T., Le, V.V., Nguyen, A.X., Nguyen, D.N. 2018. A Study On The Changes In Microstructure And Mechanical Properties Of Multi-Pass Welding Between 316 Stainless Steel And Low-Carbon Steel. *International Journal of Advanced Manufacturing Technology*, 12 (2).
- [14] Pham, X.D., Hoang, A.T., Nguyen, D.N. 2018. A Study on the Effect of the Change of Tempering Temperature on the Microstructure Transformation of Cu-Ni-Sn Alloy. *International Journal of Mechanical and Mechatronics Engineering*, 18 (4), 27-34.
- [15] Nguyen, D.N., Hoang, A.T., Sai, M.T., Chau, M.Q., Pham, V.V. 2018. Effect of Sn component on properties and microstructure Cu-Ni-Sn alloys. *Jurnal Teknologi*, 80 (6), 43-51.
- [16] Edenhofer, B., Grafen, W., Muller-Ziller, J. 2001. Plasma-carburising and surface heat treatment process for the new century. *Surface and Coatings Technology* 143-144, 335-334.
- [17] Gräfen, W., Edenhofer, B. 2005. New developments in thermo-chemical diffusion processes. *Surface & Coatings Technology*, 300, 1330-1336.
- [18] Yan, M.F., Liu, Z.R. 2001. Study on microstructure and microhardness in surface layer of 30CrMnTi steel carburised at 330oC with and without RE. *Materials Chemistry and Physics*, 73, 97-100.
- [19] Patama Visutipitukul University of Chulalongkorn, Bangkok. 2012. Nitriding of H13 Tool Steel by Direct Current Plasma.
- [20] Zagonol, L.F., Belini, Z. RLO Basso University of Sao Palou, Brazil: Nanosized Precipitation in H13 Tool Steel Low Temperature Plasma Nitriding.
- [21] Sai Ramudu Meka University STUTTGART, 2011. Nitriding of Iron based Binary and Ternary alloys: Microstructure Development during Nitride Precipitation.
- [22] Yasushiro, K., Hihara, M. 1997. Yamanashi Industrial Technology Center Kofu Yamanashi 400 Japan: Effects of Thermal Fatigue on Nitriding of Hot Working Die Steel H13.
- [23] Roloff, H., Hasler, S., Chabbi, L. University of Cambridge Material Science and Metallurgy -Cambridge CB2-UK: Multiphase Structures in Case Hardening Steel following Continuous Cooling.
- [24] Titov, N.A. 1993. Carbon potential and composition of a neutral controlled atmosphere produced from methane and a nitrogen-oxygen mixture, *Metallovedenie i Termicheskaya Obrabotka Metallov*, No.6, 10-14.
- [25] Khoroshailov, V.G., Gyulikhandanov, E.L. 1970. Saturation of steel in carburising and nitro-cementation, *Metallovedenie i Termicheskaya*

Obrabotka Metallov, No. 69, 73.

[26] Mikhailov, L.A. 1973. Calculation of the parameters of the process and the gas condition during carburising, *Metallovedenie Termicheskaya Obrabotka Metallov*, 79, 71-75.

[27] Hoang, A.T., Nguyen, D.N., Pham, V.V. 2018. Heat treatment furnace for improving the weld mechanical properties: Design and fabrication. *International Journal of Mechanical Engineering and Technology*, 9 (6), 496-506.

[28] Pham, X.D., Hoang, A.T., Nguyen, D.N., Le, V.V. 2017. Effect of Factors on the Hydrogen Composition in the Carburizing Process. *International Journal of Applied Engineering Research*, 12 (19), 8238-8244.

[29] Chieu, L.T. 2015. Carburizing, Carbonitriding and Nitriding Process, NXB BKHN.

[30] Ratajski, J., Olik, R., Suszko, T., Dobrodziej, J., Michalski, J. 2010. Design, Control and in Situ Visualization of gas nitriding Process. *Sensors*, 10, 219-240. DOI: 10.3390/s100100218.

[31] Reti, T., Czinege, I., Frelde, I., Grum, J., Ju, D.Y. 2008. Selection of tools materials for cold forming operations using a computerized decision support system. In *Proceedings of the 17th International Federation of Heat Treatment and Surface Engineering (IFHTSE) Congress, Kobe, Japan*.

[32] Burakowski, T., Wierzchoń, T. 2008. Surface engineering of metals: principles, equipment, technologies. Taylor and Francis Group, LLC: Boca Raton, FL, USA.

[33] Dobrzański, L.A., Madejski, J. 2006. Prototype of an expert system for selection of coatings for metals. *Journal of Materials Processing Technology*, 175, 163-172.

[34] Mazurkiewicz, A. 2007. Mechanisms of knowledge transformation in the area of advanced technologies of surface engineering. In *Incorporating Heat Treatment of Metals International Heat Treatment and Surface Engineering*; IOM3: London, UK, 1, 108-113.

[35] Harada, A. 1997. The framework of Kansei engineering. Report of

Modelling the Evaluation Structure of Kansei. University of Tsukuba, Tsukuba, Japan, pp. 49-55.

[36] Pitsch, W., Houdremont, E. 1956. Ein Beitrag zum System Eisen-Stickstoff. *Archiv für das Eisenhüttenwesen*, 27, 281-284.

[36] Gurov, K.P., Kartaszkin, B.A., Ugastie, J.E. 1981. Wzimmnaja Diffuzija w Mnogofaznych Sistemach; Nauka: Moscow, Russia.

[37] Ratajski, J. 2004. Model of growth kinetics of nitrided layer in the binary Fe-N system. *Zeitschrift für Metallkunde*, 95, 23-29.

[38] Dobrodziej, J., Mazurkiewicz, A., Ratajski, J., Suszko, T., Michalski, J. 2007. The methodology of fuzzy logic application in the modelling of thermally diffusive and PVD processes—Intelligent tools for support of designing in surface treatments. In *Proceedings of the International Federation of Heat Treatment and Surface Engineering (IFHTSE) Congress, Brisbane, Australia*.

[39] Frazer, B.C. 1958. Magnetic structure of Fe₄N. *Phys. Rev.*, 112, 751-754.

[40] Eickel, K.H., Pitsch, W. 1970. Magnetic Property of Hexagonal Nitride Fe_{2,3}N. *Phys. Stat. Sol.*, 39, 121-131.

[41] Heptner, H., Stroppe, H. 1965. Magnetische und magneinductive Werkstoffprüfung; VEB Deutscher Verlag für Grundstoffindustrie: Leipzig, Germany.

[42] Mittemeijer, E.J. 1984. The relation between macro-and micro stresses and mechanical. In *Proceedings of the TMS-AIME Session on Microstructural and Residual Stress Effects on the Properties of Case-Hardened steels, Warrendale, PA, USA*, 161-187.

[43] Luger, G.F. 2005. Artificial intelligence and strategies for complex problem solving. 5th ed.; Addison-Wesley: London, UK.

[44] Balakrishnan, P.A., Venkatesh, B.K. 2004. India- ASM Heatreatment Conference Chennai (Jan): Production Carbonitriding in PLG/CO₂/ NH₃ Atmosphere in batch Integral Quench Furnace.

